Pre-Launch Performance Characteristics of the Atmospheric Infrared Sounder (AIRS)

Thomas S. Pagano[a], Hartmut H. Aumann[a],
Larrabee Strow[b]

[a]California Institute of Technology
NASA Jet Propulsion Laboratory, Pasadena, CA
[b]University of Maryland Baltimore County (UMBC), Baltimore MD.

ABSTRACT

The Atmospheric Infrared Sounder represents a quantum leap in spaceborne sounding instruments with 2,378 infrared spectral channels ranging in wavelength from 3.5 to 15.5 microns. AIRS was built by NASA subcontractor Lockheed Martin Sanders (LM Sanders) in Lexington Massachusetts and is scheduled for launch on the NASA EOS-Aqua spacecraft in December 2000. Characterization of this high spectral resolution infrared spectrometer involved extensive laboratory testing in a thermal vacuum environment at cold optical temperatures. This paper summarizes the results of that testing and gives a detailed report on the spectral, radiometric and spatial performance of the AIRS. Radiometric, spectral and spatial sensitivity and accuracy predictions are presented. Based on the excellent pre-launch calibration and results of data simulation, the assimilation of AIRS data into the global forecast models is expected to result in a significant improvement in the anomalies skill score and the forecast length.

Keywords: EOS, AIRS, infrared, sounder, calibration, weather forecasting

1. BACKGROUND

The Atmospheric Infrared Sounder (AIRS) shown in Figure 1 is the first hyperspectral infrared sounder developed by the National Aeronautics and Space Administration (NASA) in support of operational weather forecasting by the National Oceanic and Atmospheric Administration (NOAA). Integration of the fully tested and calibrated AIRS flight unit with the EOS-Aqua satellite started in December 1999, with the launch scheduled for December 2000.

The AIRS instrument (shown in Figure 1) incorporates numerous advancements in infrared sensing technology to achieve a high level of measurement sensitivity, precision and accuracy. This includes long wavelength cutoff HgCdTe infrared detectors and an active pulse tube cryogenic cooler operating at approximately 60K.

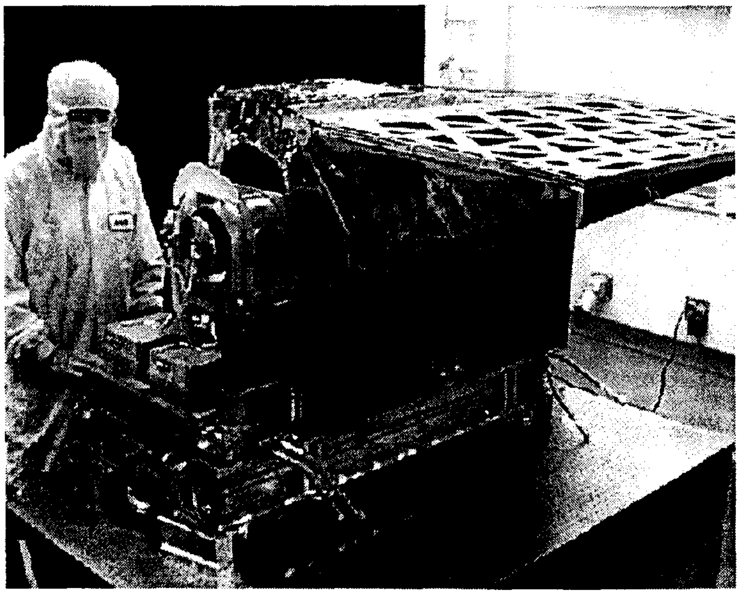

Figure 1. The Atmospheric Infrared Sounder (AIRS).

Full use of the high measurement sensitivity and accuracy capability of AIRS requires very careful prelaunch calibration. The extensive pre-launch spectral, spatial and radiometric calibration of AIRS was made using a test facility especially designed for AIRS located at Lockheed Martin Sanders facility in Lexington Massachusetts. We have previously described the AIRS hardware and provided a summary of the performance (References 1 and 2). This paper briefly reviews the AIRS measurement requirements and instrument description, then focuses on the pre-flight calibration and performance measurements of the infrared spectrometer.

2. AIRS MEASUREMENT REQUIREMENTS AND INSTRUMENT SPECIFICATIONS

The NOAA polar orbiting satellite systems have supported the operational weather forecasting with HIRS (High Resolution Infrared Sounder) and the Microwave Sounding Unit (MSU) derived global temperature and moisture soundings since the late 70's. After analyzing the impact of the first ten years of HIRS/MSU data on weather forecast accuracy, the World Meteorological Organization (WMO) in 1987 (References 3 and 4) determined that global temperature and moisture soundings with radiosonde accuracy are required to significantly improve the weather forecast. Radiosonde accuracy is equivalent to profiles with 1K rms accuracy in 1 km thick layers and humidity profiles with a 10% accuracy in the troposphere. An extensive effort of data simulation and retrieval algorithm development was required to establish instrument measurement requirements in the areas of spectral coverage, resolution, calibration, and stability, spatial response characteristics including alignment, uniformity, and measurement simultaneity, radiometric and photometric calibration and sensitivity to meet the WMO requirements. The requirements can only be met by increasing the spectral resolution of the infrared sounder by about one order of magnitude, from $\lambda/\Delta\lambda=100$ resolving power of HIRS-2 to the hyper spectral $\lambda/\Delta\lambda=1200$ resolving power of AIRS. Sensitivity requirements, expressed as Noise Equivalent Difference Temperature, NEΔT, referred to a 250K target temperature, range from 0.14K in the critical 4.2μm lower tropospheric sounding area to 0.35K in the 15 μm upper tropospheric sounding area. These requirements were captured in AIRS The Functional Requirements Document (FRD) (Ref. 5) which governed the design and development of the instrument.

AIRS, with spectral coverage from 3.7 to 15.4 μm, working together with the Advanced Microwave Sounding Unit (AMSU, 27-89 GHz) and the Microwave Humidity Sounder (HSB, 150 – 187GHz), forms a complementary sounding system for NASA's Earth Observing System (EOS), designed by NASA to support the operational weather forecasting effort of NOAA.

3. AIRS SYSTEM DESCRIPTION

The AIRS Instrument provides spectral coverage in the 3.74-4.61 μm, 6.20-8.22 μm, and 8.8-15.4 μm infrared wavebands at a nominal spectral resolution $\lambda/\Delta\lambda$ = 1200, with 2378 spectral samples. Key to the spatial coverage and the calibration is the scan head assembly, containing the scan mirror and the calibrators. A cross section of the scan head assembly is shown in Figure 2. A 360 degree rotation of the scan mirror generates a scan line of IR data every 2.667 seconds. The scan mirror motor has two speeds: During the first 2 seconds it rotates at 49.5 degrees/second, generating a scan line with 90 footprints of the earth scene, each with a 1.1 degree diameter IFOV. During the remaining 0.667 seconds the scan mirror completes one complete revolution with four independent views of cold space, one view into a 310K radiometric calibrator (called the On-Board Calibrator (OBC) Blackbody, one view into a spectral reference source (Parylene), and one view into a photometric calibrator. The VIS/NIR photometer, with a 0.185 degree IFOV, is boresighted to the IR spectrometer to allow simultaneous visible and infrared scene measurements.

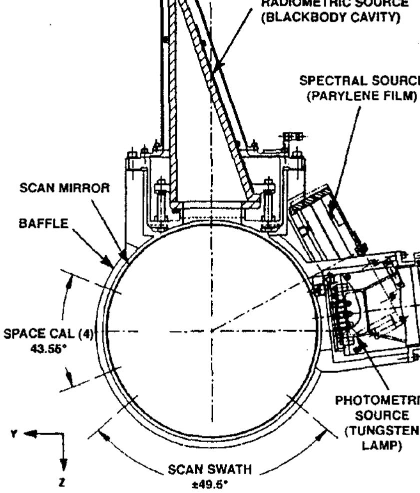

Figure 2. AIRS Scan Assembly

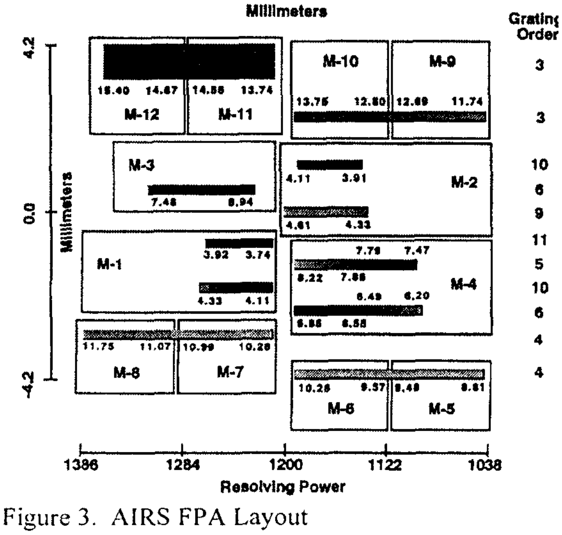

Figure 3. AIRS FPA Layout

The diffraction grating in the IR spectrometer disperses the radiation onto 17 linear arrays of HgCdTe detectors (Figure 3.) in grating orders 3 through 11. The IR spectrometer is cooled to 150K by a two stage radiative cooler. The IR focal plane is cooled to 60K by a Stirling/pulse tube cryocooler. The scan mirror is cooled to about 265K by radiative coupling to the Earth and space and to the 150K IR spectrometer. Cooling of the IR optics and detectors is necessary to achieve the required instrument sensitivity. The VIS/NIR photometer uses optical filters to define four spectral bands in the 400 nm to 1000 nm region. The VIS/NIR detectors are not cooled and operate in the 293K to 300K ambient range of the instrument housing. Signals from both the IR spectrometer and the VIS/NIR photometer are passed through onboard signal and data processing electronics, which perform functions of radiation circumvention, gain ranging and offset subtraction, signal integration, and output formatting and buffering to the high rate science data bus. In addition, the AIRS instrument contains command and control electronics whose functions include communications with the satellite platform, instrument redundancy reconfiguration, the generation of timing and control signals necessary for instrument operation, and collection of instrument engineering and housekeeping data. The Stirling/pulse tube cryocoolers are driven by separate electronics which control the phase and amplitude of the compressor moving elements to minimize vibration and to accurately control the temperature. Heat from the electronics is removed through coldplates connected to the spacecraft's heat rejection system.

4. AIRS TEST AND CALIBRATION FACILITY

A dedicated test setup was developed for AIRS to provide comprehensive characterization and evaluation of all required instrument performance parameters. The AIRS Test and Calibration Facility (ATCF) is shown in Figure 4. The ATCF includes a 2.5m x 3.5m thermal vacuum chamber in which the AIRS is mounted on a rotary stage to allow viewing of calibration targets at multiple scan angles. The primary radiometric calibration target is a Large Area Blackbody (LABB). The LABB was developed by Bomem of Canada and has an estimated calibration accuracy of 1%. Temperature sensors in the LABB have been fully calibrated and traced to NIST standards. The LABB provides full aperture illumination of the AIRS for testing of radiometric sensitivity, NEΔT, gain and nonlinearity and is the radiometric calibration standard for AIRS. Spatial and polarization testing is performed using a Spatial Collimator Source (SCS) located in a chamber external to the main chamber but linked by a gate valve. The SCS allows scanning of a point source across the AIRS field of view for spatial measurements and projection of reticals and filters such as those used for polarization measurements. Spectral measurements are made using a Brueker Fourier Transform Spectrometer (FTS) instrument with $0.1 cm^{-1}$ resolution. The FTS is coupled through the SCS to the AIRS to allow spectral measurements to be made across the field. Data are acquired from the AIRS using a Ground Support Station (GSS) computer system. Most of the analysis presented in this paper is done with MATLAB source code developed specifically for AIRS.

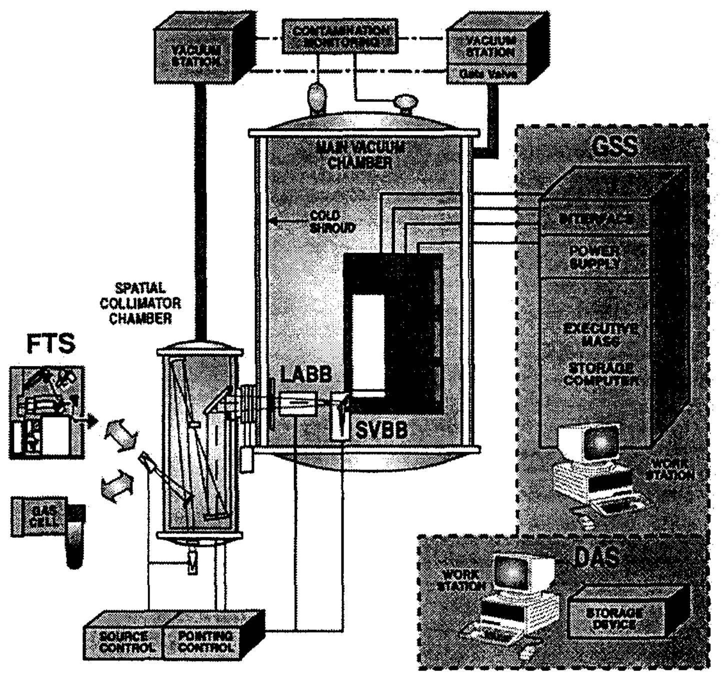

Figure 4. AIRS Test and Calibration Facility

5. PERFORMANCE MEASUREMENT RESULTS

Careful characterization of the AIRS instrument performance is necessary to provide quantitative information on the random and systematic errors that will result during the in-orbit measurement program. A comprehensive test program was developed to address all areas of the calibration and to characterize the radiometric, spatial and spectral performance of the instrument. In the following sections we will present the most recent understanding of the AIRS performance. The data are still under evaluation and we will continue to remove the systematic errors as more information is obtained.

Radiometric Test Results

Radiometric testing includes measurements of the radiometric response (DN to Radiance) and NEΔT. The radiometric response was measured by stepping the LABB over multiple temperatures: 205K, 220K, 230K, 240K, 250K, 265K 280K 295K and 310K. At each level the LABB was temperature stabilized and more than 100 scans of AIRS data acquired. The center of the LABB was carefully located and signal levels averaged over scans and available footprints.

The NEΔT results come out of analysis of the statistics of the data obtained in the LABB stepped linearity test. The NEΔT is also measured using the OBC Blackbody and has been shown to be the same as with the LABB. The NEΔT is measured at multiple temperatures but is reported primarily at 250K (see Figure 5). . The outliers in the chart are due to poorly performing detectors. These have been identified and are omitted from science retrieval processing. The data are reported on a per-spectral-resolution-element basis. In this process we have combined two adjacent spectral channels since the AIRS oversamples spectrally by a factor of 2. The NEΔT meets the requirements for most channels, however near the short wavelength end where we are photon limited, and near the longest wavelength where the detector noise is highest, we have the most difficulty. Also in the 12-13.75μm region where we are pushing the performance of the LW PV HgCdTe.

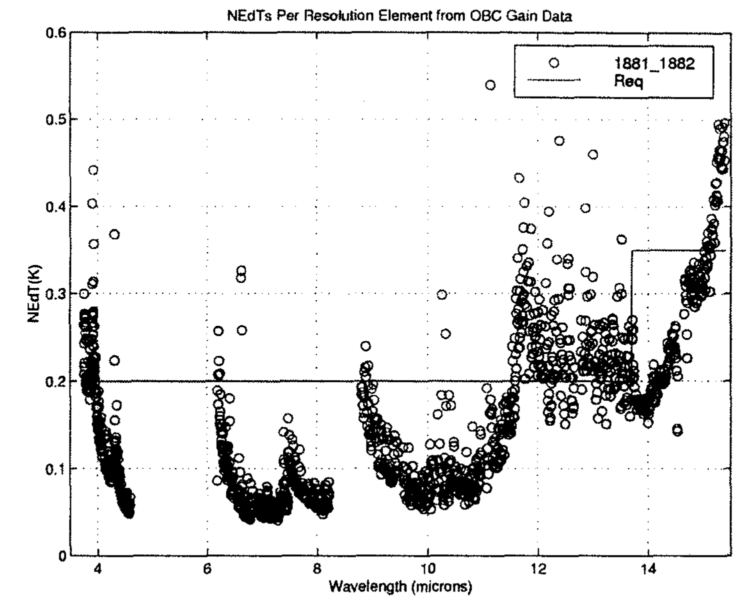

Figure 5. NEΔT for AIRS per Spectral Resolution Element.

The signal transfer curve, DN vs N (radiance) was generated from the entire data set and fit to a second order polynomial:

$$N = N_o + a_1 (dn - dn_{space}) + a_2 (dn - dn_{space})^2$$

The nonlinearity of the instrument is very small (less than 1%) as shown in Figure 6 (left). The nonlinearity was measured a second way during the thermal vacuum experiment by allowing the OBC Blackbody to cool. The OBC measurement is less accurate, but allows us a way of checking the nonlinearity in the on-orbit environment. Figure 6 (right) shows the residual errors to the fit at 230K and 250K. The results are excellent; we see less than 0.2K across the board and for most channels less than 0.1K at these critical temperatures.

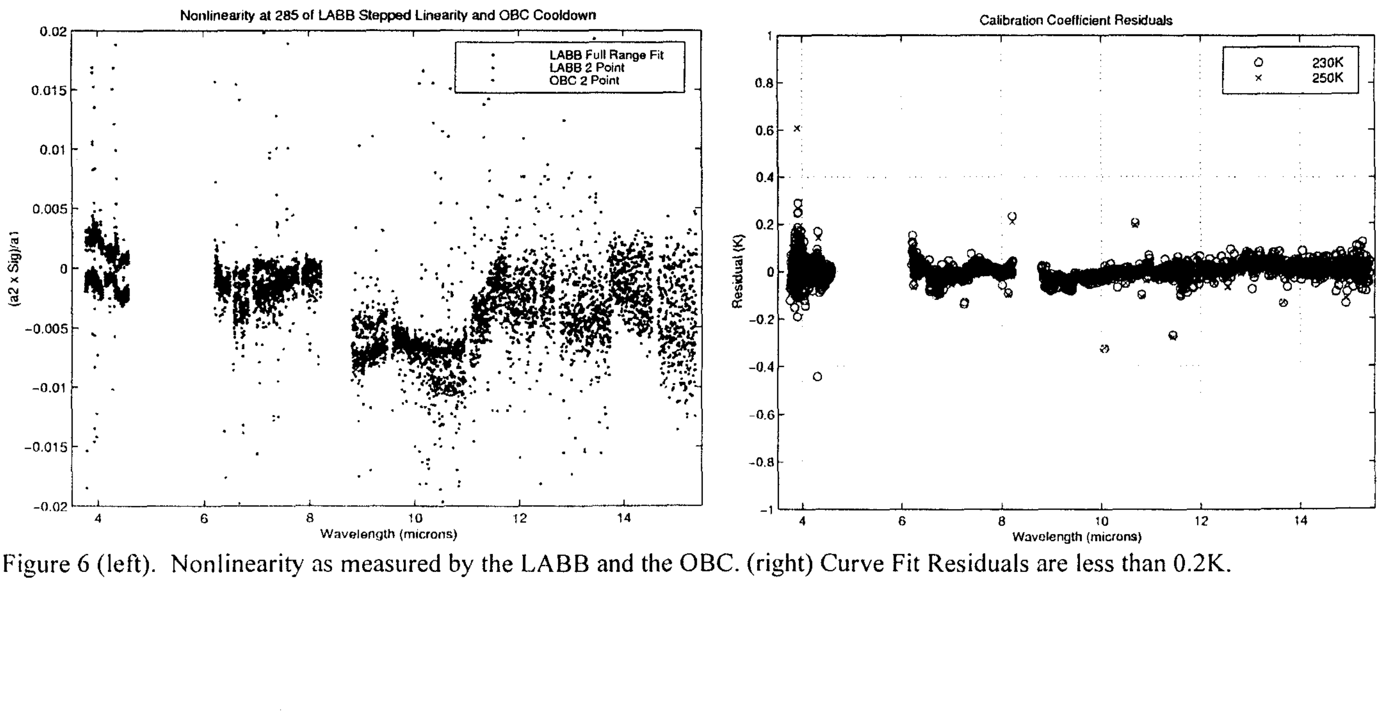

Figure 6 (left). Nonlinearity as measured by the LABB and the OBC. (right) Curve Fit Residuals are less than 0.2K.

The final figure of merit for the AIRS radiometric performance is the emissivity. When we acquire the stepped linearity data using the LABB, we simultaneously acquire data from the OBC Blackbody. We simply take the ratio of the radiance as calculated using the signals on the OBC and the coefficients from the LABB to the radiance calculated from the temperature of the OBC with a 0.3K offset. Results show excellent spectral uniformity and small residual errors.

$$\varepsilon = \frac{N_{calc}}{N_{obc}} = \frac{a_o + a_1(dn_{obc} - dn_{sv}) + a_2(dn_{obc} - dn_{sv})^2}{N_{obc}}$$

Polarization Performance

Early on in the AIRS program, it was realized that the polarization of AIRS grating spectrometer couples with the scan mirror polarization to produce a scan angle dependent radiometric modulation. This modulation is small, but not negligible and accurate quantification of the system polarization is necessary to correct the radiometry. Reference 6 discusses the conditions of the test and data acquisition of polarization data. Reference 7 discusses how these data were used to correct for the scan angle dependent radiometry.

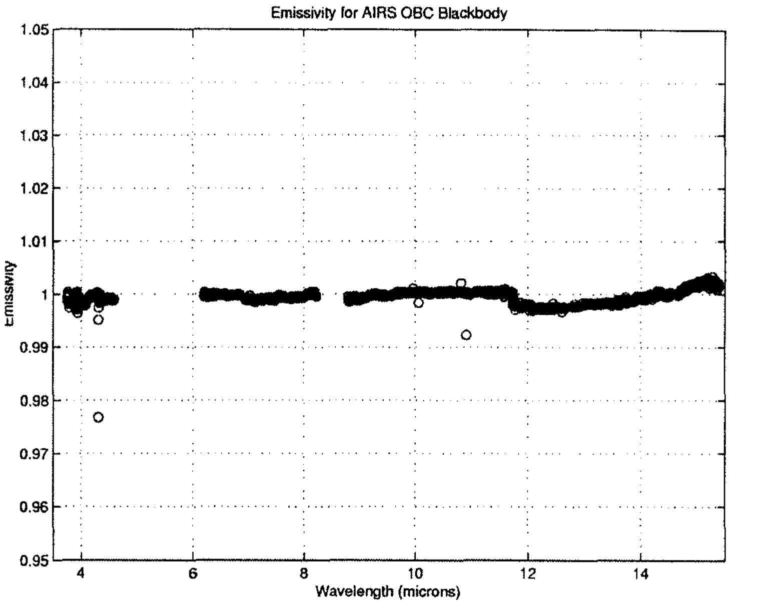

Figure 7. AIRS Emissivity is spectrally uniform to within ±0.2%.

Figure 8 (left) shows the polarization of AIRS as measured during pre-flight testing. We also show the results of a Mueler Matrix model which incorporates polarization measurements of all of the optical components in the AIRS system. We see excellent agreement for most channels. We have lesser agreement in the long wavelength modules, but attribute this to the inaccuracy of the measurement of the some componenets in the model. When we use the measured polarizations of AIRS and model the scan angle dependent effects, we get the "Modeled" results shown in Figure 8 (right) for the offset we should see at nadir due to the scan mirror being 90° from the space view. We compare the modeled result with measurements of the AIRS radiometric intercept obtained from the LABB stepped linearity test and see excellent correlation. This tells us that the radiometric offset we see at nadir is due to the modulation of the radiometry by the AIRS spectrometer and scan mirror polarization. Reference 7 gives other examples of data obtained which demonstrate our excellent knowledge of the scan angle dependent radiometric behavior of AIRS.

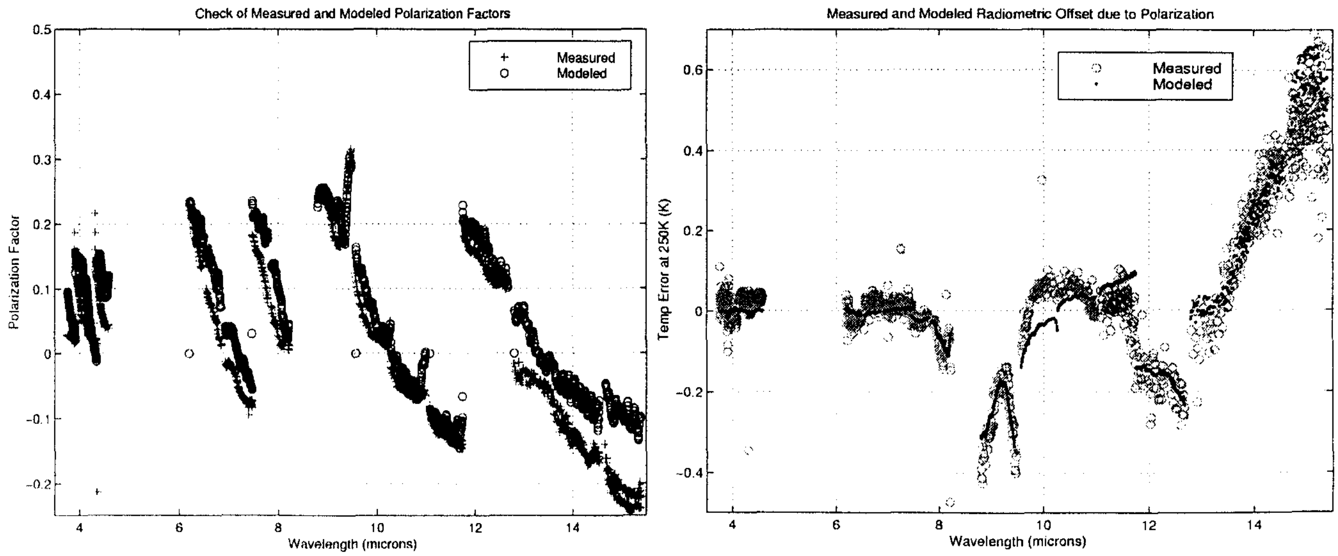

Figure 8 (left). AIRS Measured and Modeled Polarization. (right) Scan Angle Dependent Offset due to Polarization.

Spectral Response

The AIRS-Radiative Transfer Algorithm (AIRS-RTA) needs extremely accurate spectral response functions (SRFs) for each AIRS channel to ensure that the AIRS-RTA calculated radiances are within the AIRS noise level. Since AIRS retrieves atmospheric temperature and humidity profiles by comparing observed and computed radiances, the final accuracy of the AIRS products is intimately dependent on well-known SRFs.

The relevant parameters needed to characterize the SRFs are spectral centroid, width, and shape. The centroids must be known to 1% of the SRF width, the widths to 1-3% (of a width), and the shape to ≈0.1% in the wings. In practice these requirements can be relaxed significantly for channels that don't cover sharp features in the atmospheric spectrum.

Methodology

The AIRS spectral calibration utilized a very unique design where the output of a high spectral resolution Michaelson interferometer was fed into AIRS. The AIRS clock controlled the stepping of the interferometer (a Bruker), allowing AIRS to integrate the signal over 1 to n effective fields-of-view for each step of the interferometer. The final spectral calibration data was acquired with n = 6. The Bruker was run in double-sided mode, with a maximum optical path difference of 2.88 cm.

Each AIRS detector produced an interferogram, whose Fourier transform is the spectral response function (SRF) for that detector. Each interferogram was phase-corrected. Absolute wavenumber calibration was achieved by placing a gas cell containing low-pressure carbon monoxide between the interferometer and AIRS, which superimposed several carbon-monoxide absorption lines on several SRFs in the 2100 cm^{-1}spectral region. The interferogram data was zero-filled to 10 cm before taking the Fourier transform.

The AIRS entrance slit filters were not were not wedged, introducing interference fringes into the SRFs with a magnitude of ≈2-8% peak-to-peak and a period of ≈1.2 cm^{-1}. Since the SRF centroids may shift during launch, and because the SRF centroids vary with temperature differently than the phase of these fringes, we need to characterize the SRFs and fringes separately. This is easily accomplished since the Bruker SRF data is much higher resolution than the fringes. The detailed procedures are too complicated to completely describe here, but the end result is that we can accurately remove the fringe effects from the SRF for the purpose of deriving the AIRS grating model and grating spectrometer SRF shape. We have also characterized the shape of the fringes and their dependence on temperature. The final SRF used in-orbit will be the ``pure" grating SRF multiplied by the fringes, once their phase is known in orbit. (We can compute the fringe phase from the entrance filter temperature.) The following discussion on the SRFs and grating model refers to the ``de-fringed" SRFs.

Grating Model

The AIRS grating model starts with the standard grating equation,

$$m\,\lambda = d\,(\sin(\theta_i) + \sin(\theta_d))$$

where m is the grating order, λ the wavelength, d = 77.560 μm is the groove spacing, θ_i the angle of incidence and θ_d the angle of diffraction. AIRS has two incident angles, θ_i = 0.55278, 0.56423 radians due to the use of two entrance slit planes in the spectrometer. The diffraction angle can be expressed in terms of the detector position on the focal plane using

$$\theta_d(k,i) = \tan^{-1}(y^k_i / F)$$

where y^k_i is the position of the i_{th} detector in the k_{th} array in the focal plan, and F is the focal length of the focusing mirror. Each AIRS detector is separated by a known distance of 50 μm. These leaves us with two remaining parameters to determine from the spectral calibration data for each of the 17 AIRS arrays; (1) the effective focal length F, and (2) the ``starting position" of the first detector in each array, which we will call y^k_o. A non-linear least-squares fit for these two parameters for each array used data from all good tests and channels, including both the A- and B-side detectors. The residuals of these fits exhibited some small systematic errors for some arrays, with a maximum error corresponding to 1-2% of a width. Consequently, our final grating model included a small quadratic term that removes this small systematic error.

The variation of the SRF centroids between different tests, and between the A- and B-side detectors is within our specification (1% of a width), although we can detect A- to B-side shifts. In orbit we will generally use an almost equal combination of A- and B-side signals (called ``Opt") for the channel radiance, so averaging all A- and B-side tests together for the grating model will be sufficiently accurate. Figure 9 shows the deviations of the grating model fits from the mean of all tests for the T = 161K calibration tests. This figure highlights the sensitivity of the spectral calibration test setup and the high signal-to-noise of these measurements. The array position were found to vary slightly with temperature by an amount equivalent to a centroid shift of 2.2% of a width per K. The effective focal lengths F, did not exhibit any dependence on temperature.

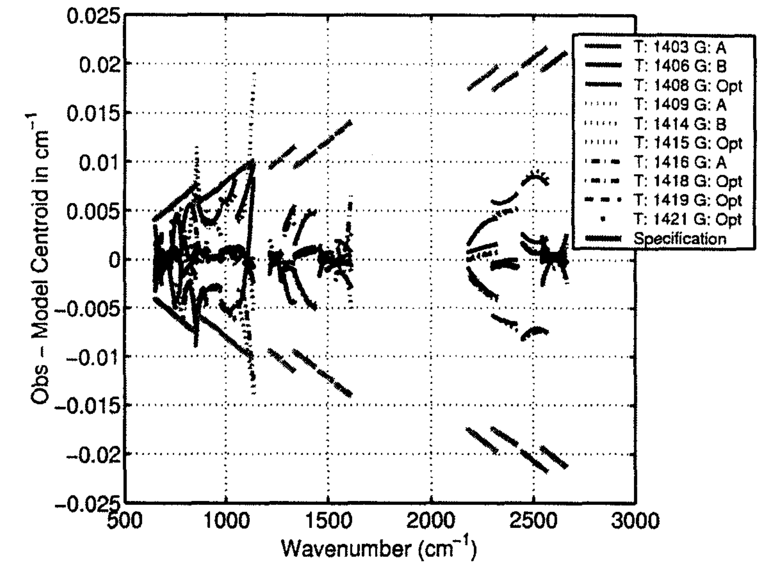

Figure 9: Deviation of centroids from test mean, T = 161K

SRF Width and Shape

The SRF width measurements showed no variation with temperature, and were determined to the required specs (1-3%) or better. The observed widths were found to be 3-14% *narrower* than expected, which is a curious result given that the SRF widths are almost totally determined by the combination of the grating dispersion and the entrance slit widths. Figure 10 shows measured SRFs averaged over three broad wavenumber ranges. These are averages of channels over several arrays, nominally ~ 5-6 arrays per average. The SRFs are nominally 100 microns wide, so this figure shows that the SRF magnitude is below 0.1% of its peak value at 3 full widths from the channel center.

The observed SRFs were fit to a simple analytic function (roughly the sum of a Lorentz plus a Gaussian shape) with good results. Our main goal for these fits was to smooth noise in the SRF wing. These fits included the effects of the Bruker, which introduces very noticeable sinc ringing in the longest wave arrays. Variations of the SRFs within a single array is undetectable and below our specifications, allowing us to use a single shape (but not width) for each channel in each array. Variations in the SRF shape among arrays is also quite small, but big enough that we need to take them into account.

All results presented were acquired after insertion of a field mask at the field stop of the telescope. This field mask was inserted to reduce field dependent spectral sensitivity, but cost the system 35% in signal. The tradeoff worked and we now have the spectral uniformity across the field as desired.

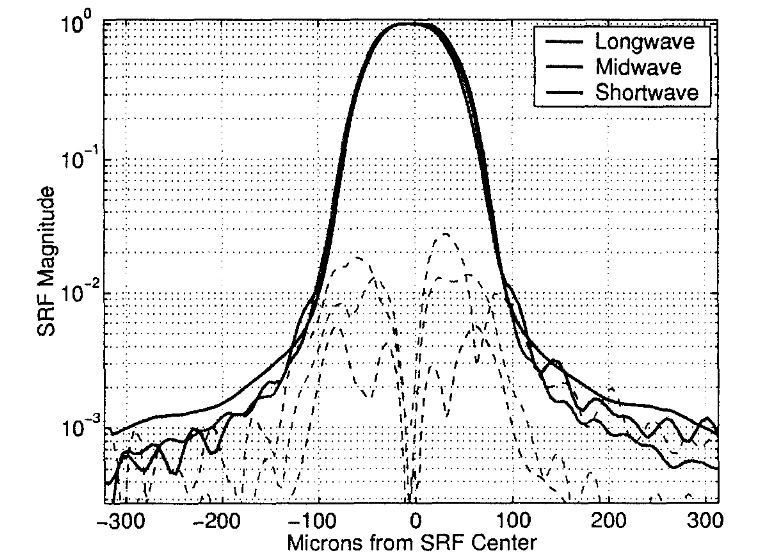

Figure 10: Observed SRFs averaged for three broad wavenumber regions The dashed lines are the standard deviation of these averages.

Air-gap Spectra

An independent verification of the spectral calibration data was made by using AIRS to measure spectra of the laboratory air in regions of strong $CO_2$and H_2Oabsorption. Using a combination of blackbody temperatures and placements in the room, we were able to measure the ratio $\tau_{25}/\tau_{2.5}$ where τ_L is the AIRS convolved transmittance of the room air for a path of L inches. Measurements were taken at all 3 calibration temperatures.

Figure 11 is an example of this measured ratio in a region of strong absorption by CO_2 in the laboratory air. We fit the air-gap spectra to the known CO_2 absorption in this region, letting the following parameters float; (1) CO_2 amount, (2) the AIRS array offset (y^k_o), and (3) a single multiplier for the SRF width for all channels. Both y^k_o and the width multiplier agreed with values derived from the interferometer spectral calibration, to within our required specifications. This result gives us great faith in the rather complicated interferometer calibration system, since it is totally independent of that system and is an absolute calibration tied to extremely well known molecular spectroscopy.

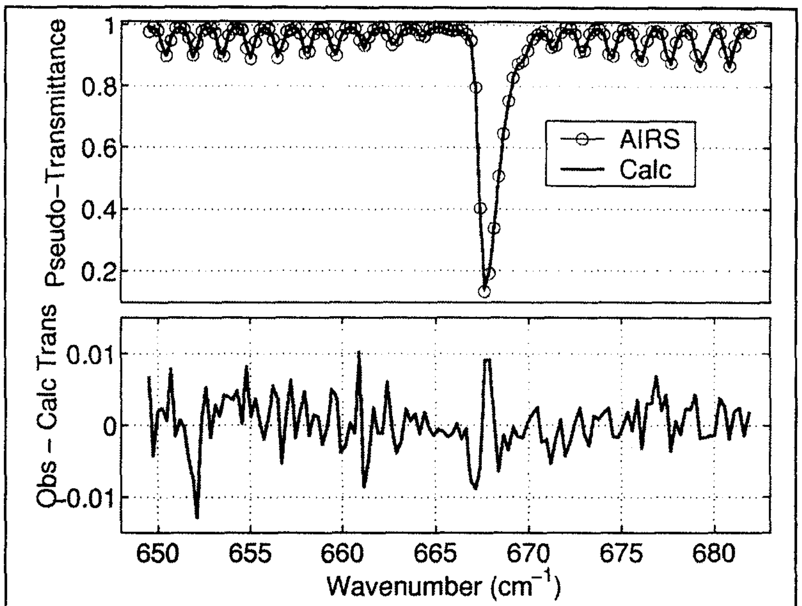

Figure 11: CO_2 spectrum taken with AIRS.

Spatial Response

Near Field Response

The AIRS spatial response was measured using the SCS. In this experiment, a 0.1° circular spot was scanned in two dimensions across the 1.1° field of view of the AIRS. The AIRS response was measured for all of the 2378 channels. Examples of these response profiles are shown in Figure 12 (left). The profiles shown here were obtained prior to insertion of the field mask discussed above, and do not include the scanning motion of the instrument. Limited data sets were obtained to verify that a simulation of the resulting spatial response with the field mask in place were valid. We then used the simulation software to compute the co-registration of the AIRS reference channels (3 channels near center and two ends of each of the 17 modules). A figure of merit of the coregistration is the C_{ij}, where

$$C_{ij} = 1 - (\iint | s_i - s_j | \,dx\,dy)/(\iint s_i \,dx\,dy + \iint s_j \,dx\,dy),$$

where $s_k = s_k(x,y)$ is the two dimensional spatial response function of the k^{th} IR spectral channel, including the cross-track scan motion. Figure 12 (right) shows the C_{ij} for the 51 reference detectors. The C_{ij} does not meet the original requirements set forth in the FRD (reference 5), however, algorithmic techniques will be implemented in the science data processing software to mitigate the noncompliance.

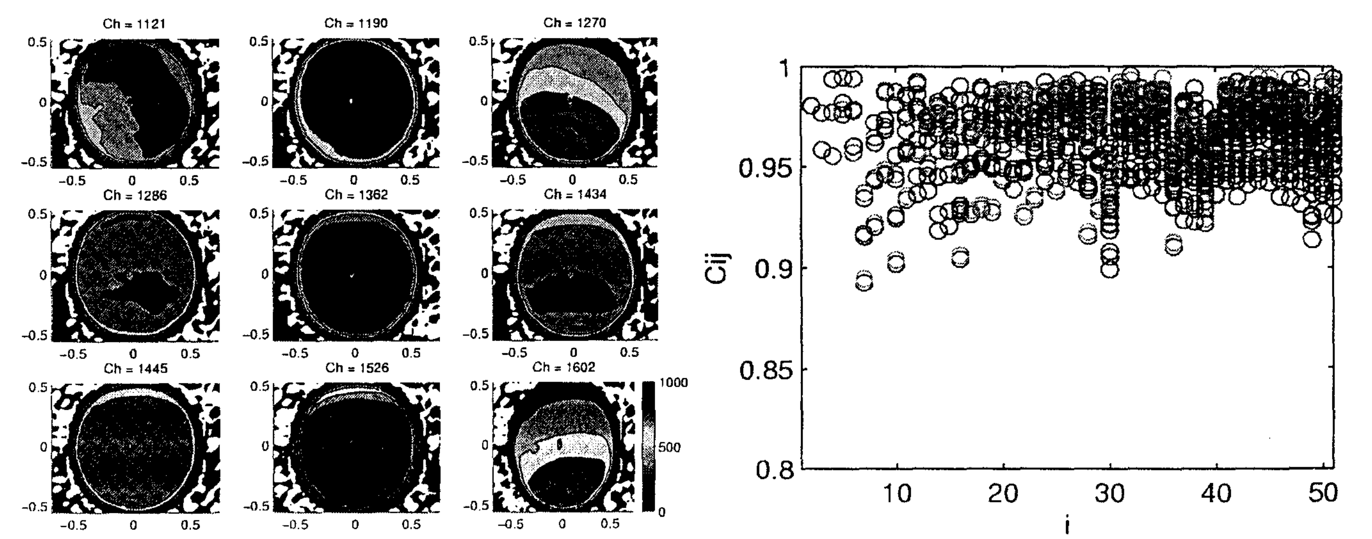

Figure 11 (left). Static Scan Spatial Response of AIRS Channels. (right). Simulated Cij, scanning with field mask

Far Field Response

The FRD requires that 99% of the encircled energy of the instrument be contained within the first 2.5 degrees. The far field response of the AIRS was measured using a 0.2° spot scanned in the same way as for the C_{ij} test. Figure 12 shows a typical response function obtained from this test. The data are plotted on a log scale.

For this analysis, the worst response of all the modules was used in an extrapolation. The wings of the response were fit to a 2nd order polynomial which goes to zero at ±3°. The encircled energy calculation within the first 2.5° captured more than 99.9% of the energy and we believe there is considerable margin to this requirement.

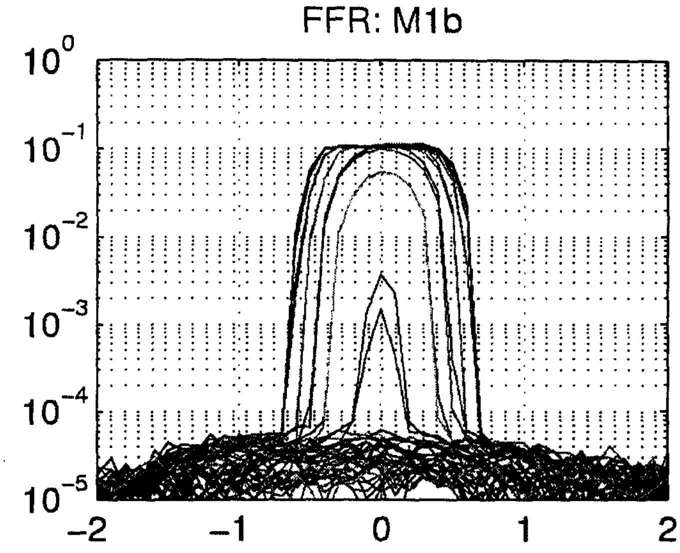

Figure 12. AIRS far field response vs azimuth at multiple elevation positions. We see good rejection to below 10^{-4} in response.

6. SUMMARY

The AIRS instrument represents a major advance in passive IR remote sensing technology. The extensive spectral, spatial and radiometric calibration effort demonstrate the high measurement accuracy and stability of AIRS. The AIRS derived data about the atmosphere, land and oceans will be of unprecedented accuracy to support the operational weather prediction effort of NOAA and climate and global change research objectives of NASA.

7. ACKNOWLEDGMENTS

The AIRS instrument was designed, built and tested by Lockheed/Sanders Infrared and Imaging Systems (LIRIS), Lexington MA, under a systems contract with the Jet Propulsion Laboratory, Pasadena, CA. The calibration data analysis was the combined effort of the calibration team, with members form Lockheed, JPL and the AIRS science team. The Jet Propulsion Laboratory, California Institute of Technology, operates under contract with the National Aeronautics and Space Administration.

REFERENCES

1. "Atmospheric Infrared Sounder (AIRS) on the EOS Observing System", H. H. Aumann and Chris Miller, SPIE Vol.2583, pp 332-343 (1995).
2. "Development and test of the Atmospheric Infrared Sounder (AIRS) for the NASA Earth Observing System (EOS).", P. Morse, J. Bates, C. Miller, SPIE 3759-27, July 1999.
3. "The World Weather Watch Programme 1988-1997", World Meteorological Organization, WMO-No.691 (1987)
4. "Inference of atmospheric structures from satellite remote radiation measurements", L. D. Kaplan, J. Opt. Soc. Am., Vol. 49, pp 1004-2007 , 1959.
5. "AIRS Functional Requirements Document", JPL Internal Document D- 8236, Rev.1., Oct.1992.
6. "AIRS instrument polarization response: measurement methodology, G. Gigioli and T. Pagano, SPIE 3759-30, July 1999
7. "Scan Angle Dependent Radiometric Modulation due to Polarization for the Atmospheric Infrared Sounder (AIRS)", T. Pagano, et. al, SPIE 4135-14, In Print August 2000.